Journal of Low Temperature Physics, Vol. 123, Nos. 1/2, 2001

Dynamics of a Charged Fluctuator in an Al–AlO_x–Al Single-Electron Transistor

M. Kenyon,[1,*] J. L. Cobb,[2,†] A. Amar,[1,‡] D. Song,[1,§]
N. M. Zimmerman,[2] C. J. Lobb,[1] and F. C. Wellstood[1]

[1] *Center for Superconductivity Research, Department of Physics, University of Maryland, College Park, Maryland 20742-4111*
[2] *National Institute of Standards and Technology, Gaithersburg, Maryland 20899*

(Received November 18, 2000)

We report detailed observations of random-telegraph charge fluctuations in a two-junction Al–AlO_x–Al single-electron transistor (SET). We measured the fluctuations from 85 mK to 3 K and observed that the SET switched between two states, causing charge shifts of $\Delta Q_o = 0.1 \pm 0.02$ e on the SET's island. The transition rate out of each state was periodic in the gate voltage, varied non-monotonically with the device bias voltage, and was independent of the temperature below about 0.3 K. We discuss two effects which could contribute to the behavior of the transition rates, including heating of the defect by the island conduction electrons and inelastic scattering between the defect and electrons flowing through the SET.

1. INTRODUCTION

Charge offset, extrinsic low-frequency charge noise, and drift seriously limit the practical use of single-electron transistors (SETs) in potential applications such as capacitance standards,[1,2] memory storage devices,[3] and quantum computers.[4,5] Although it is clear that the noise is due to the movement of charges in dielectric materials within or near the device, many questions exist regarding the microscopic nature, location, and dynamics of the moving charges. For example, is the noise due to the actual motion of ions, the reconfiguration of electronic states, or the trapping and untrapping of electrons? Are the moving charges located in the tunnel junctions, substrate surface, or metal-substrate interface? Are the charges in thermal

*E-mail: mkenyon@squid.umd.edu
†Current address: Motorola, Inc. Austin, Texas 78721.
‡Current address: IBM, Almaden Research Center, San Jose, California 95120.
§Current address: Seagate Technology, Inc. Bloomington, Minnesota 55435.

0022-2291/01/0400-0103$19.50/0

equilibrium, undergoing quantum tunneling, or being driven by external sources?

In some SETS, telegraph noise from distinct two-level fluctuators (TLFs) are clearly evident, showing up as sudden charge shifts in the device characteristics (see Fig. 1a). By studying individual TLFs for different bias conditions and temperature, one can begin to answer questions about the moving charges present in SETs. Other systems where TLFs have been systematically studied using such techniques include MOSFETs,[6] nanobridges,[7] and ultrasmall tunnel junctions.[8] Here, we report on the detailed behavior of a distinct two-level charge fluctuator in a normal metal Al–AlO_x–Al SET.

According to the Orthodox Theory of Averin and Likharev,[9] the current I flowing through the device will change if the polarization charge of the island changes due to nearby gates or charged objects. For example, changing the voltage V_g applied to a gate electrode near the SET's island changes the induced polarization charge on the island by $C_g V_g$, where C_g is the capacitance of the gate to the island (see Fig. 1b). Similarly, a moving background charge, residing in the dielectric materials within or near the SET, can also couple electrostatically to the island and cause I to change appreciably.

In principle, even a single ion hopping between two states separated by a fraction of a nanometer can produce a significant induced polarization charge shift in an SET. The size of the induced polarization charge shift depends on several factors, including the ion's location, the hopping displacement, and the charge of the ion. The transition rate out of either state will generally be a strong function of the energy barrier that separates the two states. Since an ion is charged, the height of this barrier can be modified by voltages which are applied to the SET. Thus, one expects the transition rates may be strongly dependent on the gate voltage V_g and the voltage across the device V_b. In addition, the transition rates can be affected by phonons and electrons which are flowing through the SET. By systematically studying how the transition rates depend on applied bias voltages and temperature, one can infer a considerable amount about the microscopic nature of the moving charge.

We begin by describing our experimental procedure and our measurement results. We next draw some broad conclusions. We then examine our results in terms of two detailed models which assume that either defect heating caused by island self-heating or inelastic scattering between the defect and electrons tunneling through one of the junctions strongly determine the behavior of the fluctuator. Finally, we use the results of the inelastic scattering model to infer the microscopic nature of the charged defect; i.e., whether the fluctuations are due to an ion or electron hopping

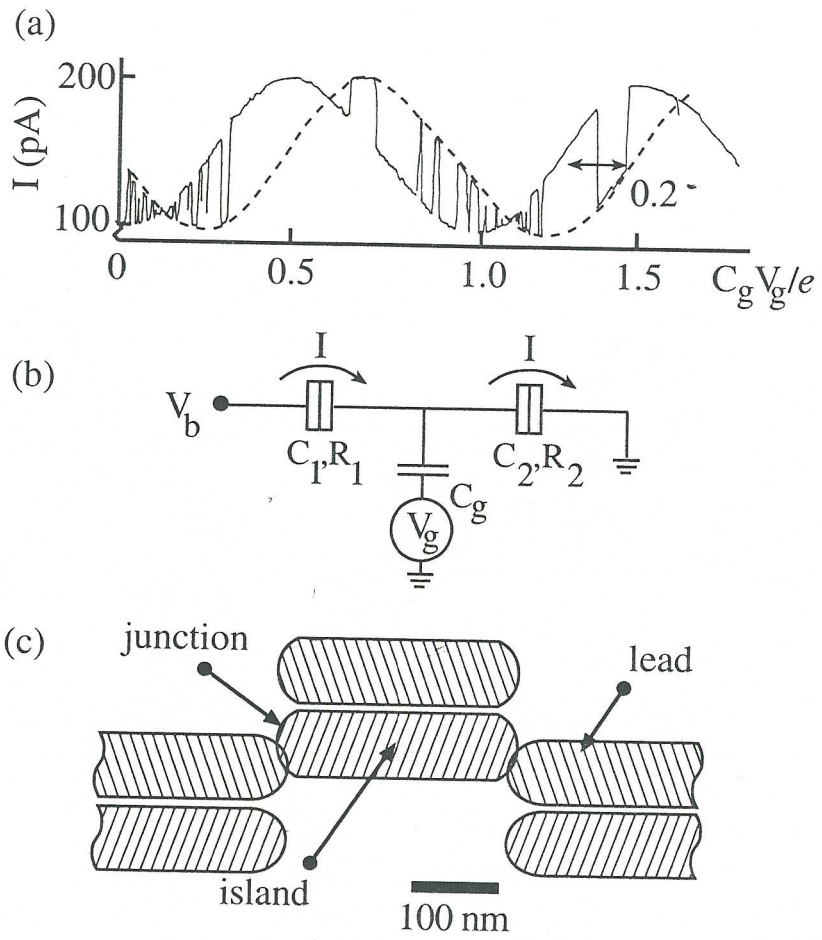

Fig. 1. (a) $I-V_g$ characteristic of an Al–AlO_x–Al SET with prominent charge fluctuator. The fluctuator ($F1$) is characterized by τ_1 and τ_2 which are the mean lifetimes the SET spends in state 1 (dashed curve) and state 2 (solid curve), respectively. The SET switches at random times as V_g is swept, causing the island charge to shift by 0.2. Note: the device shown here is different than the one discussed in detail in later sections. (b) SET schematic. The boxes represent ultra-small Al–AlO_x–Al tunnel junctions with capacitances C_1 and C_2 which separate the leads from the island. (c) Configuration of SET with an in-line layout. The hatched region in the drawing represents Al. The top island and bottom leads are byproducts of the double-angle evaporation. (The gate is not visible in the drawing).

between two localized states or the charging and discharging of an electron trap.

EXPERIMENTAL PROCEDURE

While all SETs show excess charge noise, we have found just two devices which displayed clear, distinct, two-level fluctuators in the $(I-V_g)$ characteristics. One device showed a prominent fluctuator which we will label $F1$ with $\Delta Q_o \simeq 0.2\,e$ (see Fig. 1a). Unfortunately, this switcher was only visible over a small temperature range and was rather slow, making it difficult to obtain a good characterization of the switching behavior for many different device bias conditions. The second device showed a prominent two-level fluctuator which we will label $F2$ with $\Delta Q_o = 0.1 \pm 0.025\,e$ over a temperature range from about 85 mK to 3 K. Furthermore, the switching speed of $F2$ was typically in the range of 1 Hz to 1 kHz, making for easy and relatively rapid data collection.

The latter Al–AlO_x–Al SET was fabricated on a Si wafer which was coated with 0.5 μm of thermally grown SiO_2. We used standard e-beam lithography and double-angle shadow evaporation[10] to construct the device. The SET had an in-line geometry with an island length of about 0.25 μm, a width of about 0.1 μm and a thickness of about 20 nm (see Fig. 1c). We measured the current versus bias voltage $(I-V_b)$ and current versus gate voltage $(I-V_g)$ characteristics of the device while it was mounted on the mixing chamber of a commercial dilution refrigerator. We applied a field of 0.5 T to keep the device in the normal state during the measurements. The refrigerator was enclosed in an rf-shielded room and all leads to the dewar were heavily filtered at the cryogenic end to minimize external noise.[11] From the measured characteristics, we were able to determine the parameters of the SET: tunnel junction capacitances $C_1 = C_2 =$ 62 aF, gate capacitance $C_g = 1.85$ aF, and junction resistances $R_1 = R_2 =$ 315 kΩ. We note that these values of C_1 and C_2 imply an overlap area of roughly 25×25 nm. The island capacitance was $C_\Sigma = C_1 + C_2 + C_g =$ 126 aF. The relatively small island capacitance of the SET allowed us to make measurements up to several kelvin. For example, the device still showed about 45 pA of current modulation at 4.2 K.[12]

To fully characterize the behavior of the two-level fluctuator $F2$ in this SET, we determined the transition rate out of each state as a function of the gate voltage V_g, the bias voltage V_b, and the temperature T.[13] For convenience we will label the two charge states of $F2$ as state 1 and state 2. To measure the transition rates $1/\tau_1$ and $1/\tau_2$ out of state 1 and state 2, respectively, we fixed V_b, V_g, and T and recorded the current through the SET as a function of time (see Fig. 2). Typically, we measured long enough

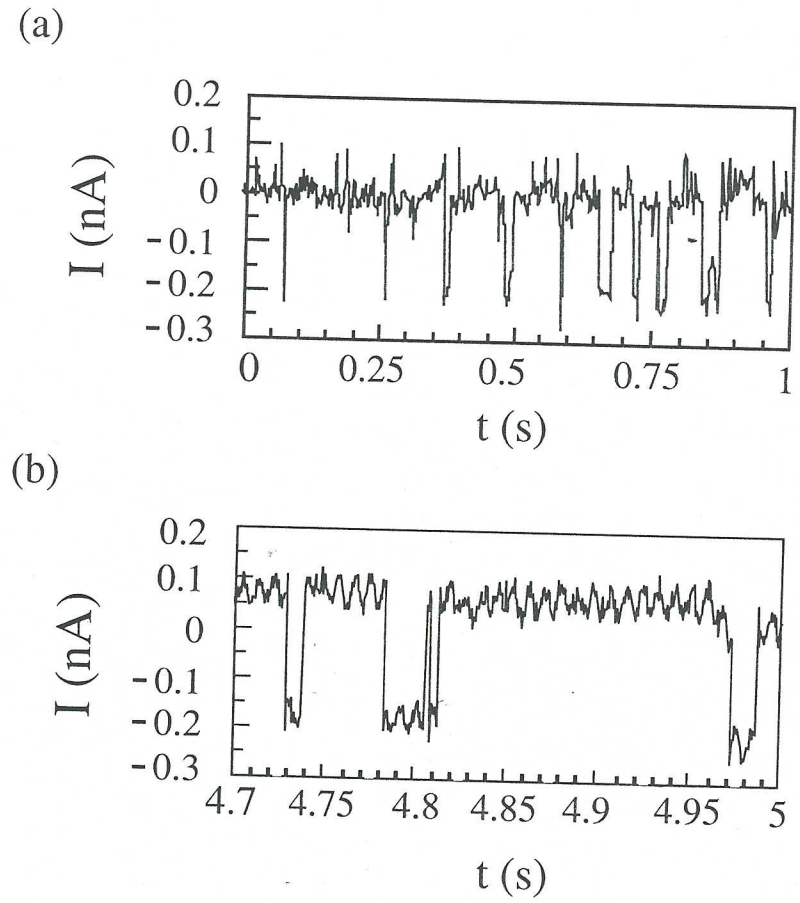

Fig. 2. (a) Current versus time. The fluctuations cause the current through the SET to change by about ± 0.2 nA. For this measurement, the temperature is 1.1 K, $V_g = 0.37\ e/C_g$, and $V_b = -1$ mV. (b) A current record over a shorter time showing that the SET switches between two charge states. Other low-frequency noise is clearly visible.

to observe several hundred switching events. We note that the bandwidth of our system did not allow us to measure times much less than 1 ms, limiting us to a maximum temperature of about 3 K for this TLF.

It is worth noting that our measurements of charge fluctuations in SETs differ considerably from many previous measurements of fluctuations in other non-SET systems. For example, other groups have measured resistance fluctuations in junctions or bridges.[6-8] In these systems, the

devices are current biased and voltage fluctuations are measured. These fluctuations are due to changes in the tunnel barrier or tunnel resistance of the device. In contrast, we fix the bias voltages and observe changes in the SET current which are caused by shifts in the induced polarization island charge, not shifts in the junction resistance. Although at first sight this might appear to be similar to a technique which measures resistance fluctuations, in fact inspection of $I-V_g$ curves like the one shown in Fig. 1a clearly reveal that our TLFs are causing the induced polarization island charge to change while the junction resistance remains constant.

MAIN EXPERIMENTAL RESULTS

We now discuss the main features in the data for our SETs. Analysis of time records such as Fig. 2 reveal that the switching process is random. In particular, the probability P_i for the system to remain in state i is governed by the distribution $P_i \propto \exp^{-t/\tau_i}$ where $1/\tau_i$ is the transition rate out of state i. Figure 3a shows the measured transition rates of $F2$ versus temperature for $V_b = 1.2$ mV and $V_g = 0.8\ e/C_g$. As expected, the transition rates tend to increase as the temperature increases. However, one sees that $1/\tau_1$, the rate out of state 1, is independent of temperature below about 300 mK, and the rate $1/\tau_2$ out of state 2 becomes independent of T below about 500 mK.

Examination of Fig. 3a also shows that over the entire temperature range $1/\tau_2 > 1/\tau_1$; i.e., at any temperature the system spends more time in state 1 than state 2. This suggests that state 2 has a higher energy than state 1. To verify this, we can plot the ratio τ_2/τ_1 versus $1/T$ (see Fig. 3b). If the fluctuator were in thermal equilibrium, then the ratio τ_2/τ_1 would obey Boltzman statistics, i.e., $\tau_2/\tau_1 = n_2/n_1 \exp(-\Delta E/(k_b T))$ where ΔE is the energy difference between state 2 and state 1 and n_i is the degeneracy of state i. Thus, we expect that a semilog plot of τ_2/τ_1 versus $1/T$ should yield a straight line. Since the data in Fig. 3b does not fall on a straight line, this suggests that below about 600 mK the fluctuator is not in thermal equilibrium with the bath. Similar results were observed when $V_b < 0$. It is also interesting to note that the ratio τ_2/τ_1 appears to approach unity as $1/T$ goes to zero (see dashed line in Fig. 3b). This suggests that the degeneracy of state 1 is the same as the degeneracy of state 2.

Figure 4a shows how the rates of $F2$ depend on gate voltage V_g at $T = 0.134$ K and $V_b = 1.3$ mV. We observe a clear periodicity, with the maximum transition rates out of state 1 occurring at slightly higher gate voltages than the corresponding maximum rates out of state 2. To test how the periodicity is affected over a large range of gate voltages, the gate voltages used to determine the ten data points comprising the left peak in

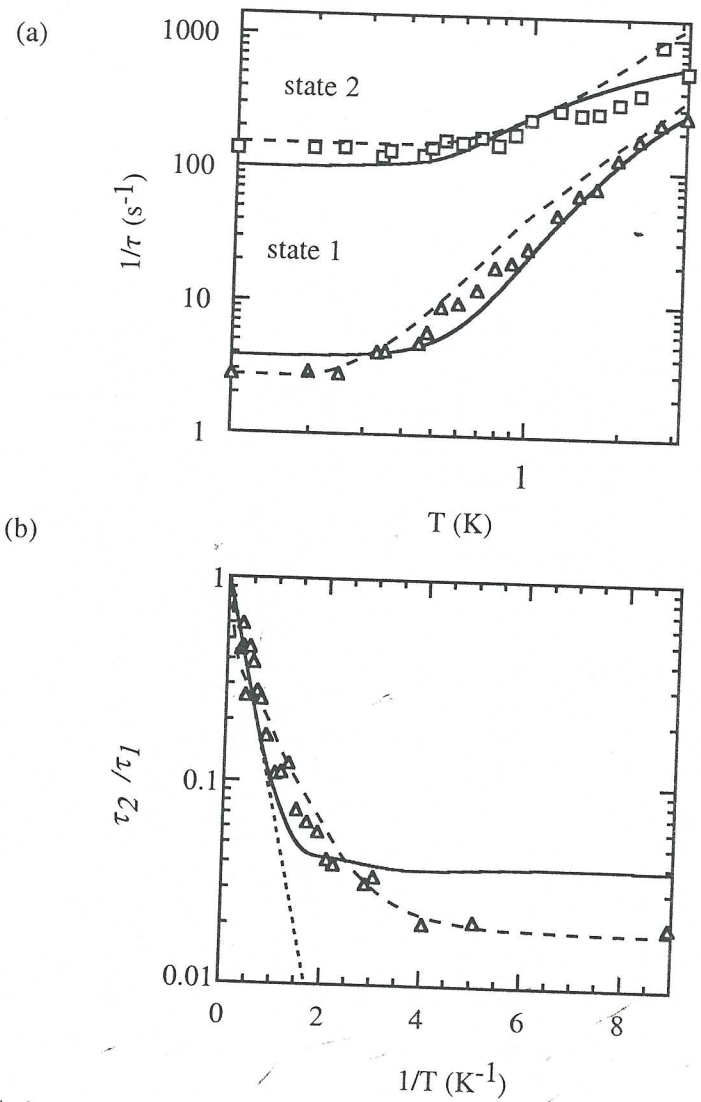

Fig. 3. (a) Open points show measured rates $1/\tau_1$ and $1/\tau_2$ of $F2$ versus T. The dashed and solid lines are simulations of the inelastic scattering and island self-heating models, respectively. $1/\tau_1$ and $1/\tau_2$ correspond to △ and □, respectively, and were taken with the bias and gate voltages set to $V_b = 1.2$ mV and $V_g = 0.8\ e/C_g$. (b) Ratio τ_2/τ_1 versus $1/T$ for the data in (a). The short dashed line indicates the functional dependence of the ratio one expects if the TLF were in thermal equilibrium with the bath. The dashed and solid lines are results from the inelastic scattering and island self-heating models, respectively.

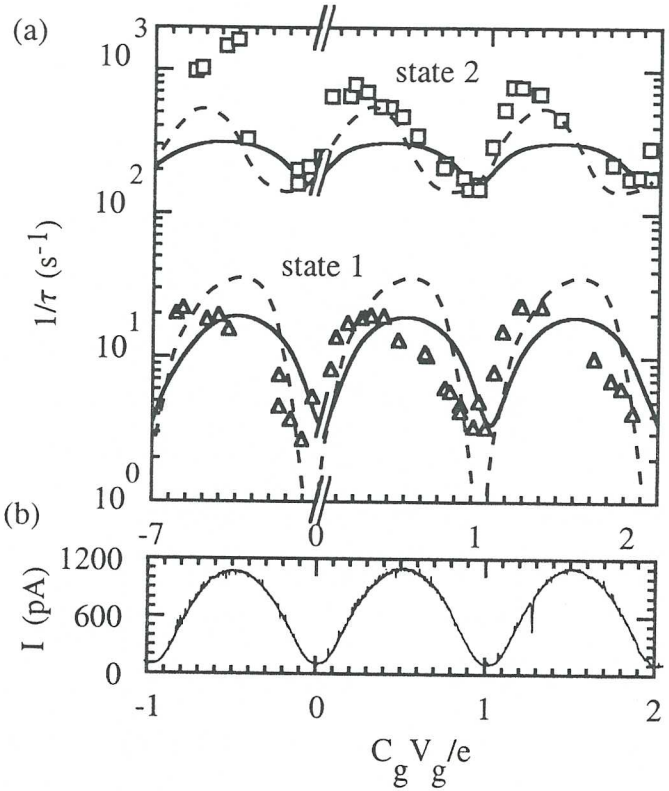

Fig. 4. (a) The rates $1/\tau_1$ and $1/\tau_2$ of $F2$ versus $C_g V_g/e$. $1/\tau_1$ and $1/\tau_2$ correspond to △ and □, respectively. The data were taken with $V_b =$ 1.3 mV and $T = 0.134$ K. The solid lines are island self-heating model simulations. The dashed lines are simulations from the inelastic scattering model. Note that the gate voltages used to determine the ten data points comprising the left peak are lower by a value of 7 e/C_g than the gate voltages used to collect the data in the other two peaks. (b) Measured I versus $C_g V_g/e$ curve when $T = 0.09$ K and $V_b = 1.2$ meV.

Fig. 4a were lower by a value of 7 e/C_g than the gate voltages used to collect the data in the other two peaks in Fig. 4a. While there is scatter in the data, the periodicity is quite striking. We also note that the maximum and minimum rates do not precisely coincide with the maxima or minima of the $I - V_g$ characteristic (see Fig. 4(b)). Finally, we observed periodic transition rates versus V_g in the two-level fluctuator $F1$ displayed in Fig. 1(a). These rates are much slower and reach their maxima and minima values for different gate voltages (see Fig. 5).

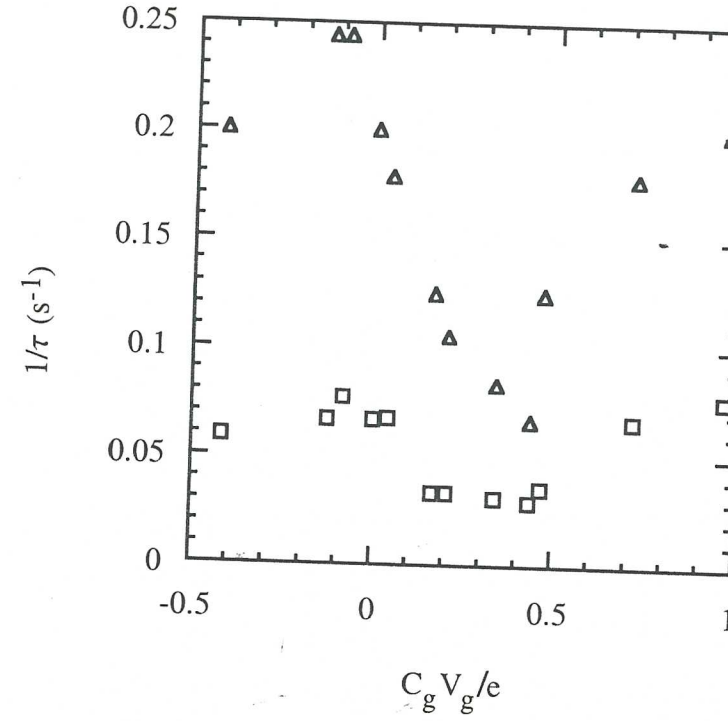

Fig. 5. (a) The rates $1/\tau_1$ and $1/\tau_2$ versus $C_g V_g/e$ for $F1$. $1/\tau_1$ and $1/\tau_2$ correspond to △ and □, respectively. The data were taken with $V_b = -136$ μV and $T = 0.06$ K. The device parameters for this defect were $C_1 = C_2 = 510$ aF, $C_g =$ 40 aF, and $R_1 = R_2 = 65$ kΩ. We note that this device was fabricated and measured in a similar way to the device discussed in Figs. 3, 4, and 6, but since the transition rates were slow and the junctions large, we were unable to obtain extensive data as a function of bias voltage and temperature.

Finally, Fig. 6 shows how $1/\tau_1$ and $1/\tau_2$ of $F2$ vary when we fix the gate voltage and the temperature and vary V_b. The gate voltage was fixed over a range of $V_g = 0.2$ e/C_g to 0.4 e/C_g and the temperature was fixed at $T = 0.09$ K when $V_b < 0$. When $V_b > 0$, the gate voltage was set between $V_g = 0.3$ e/C_g and 0.4 e/C_g, and $T = 0.13$ K. We observe that the rate $1/\tau_1$ varies non-monotonically with V_b and decreases rapidly as $|V_b| \to 0$. As discussed below, this is surprising because it is not consistent with a simple tilting of a barrier. The transition rate out of the higher energy state $1/\tau_2$ is quite different; it does not appear to go to zero as $V_b \to 0$, but instead appears to approach a minimum value of about 130 s^{-1}. Again, this behavior is not consistent with simple tilting of a barrier.

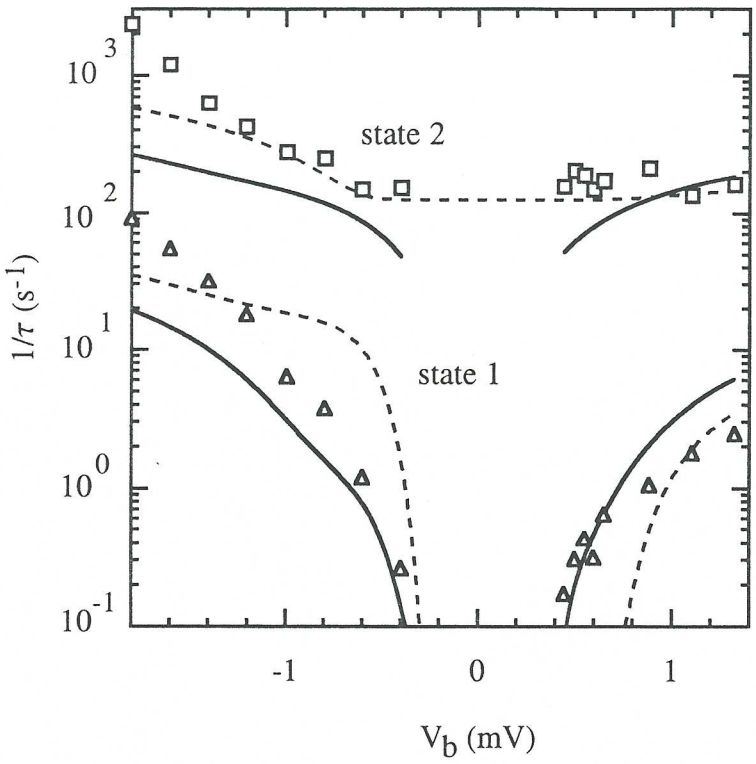

Fig. 6. The rates $1/\tau_1$ and $1/\tau_2$ versus V_b. $1/\tau_1$ and $1/\tau_2$ correspond to △ and □, respectively. The gate voltage was fixed over a range of $V_g = 0.2\ e/C_g$ to $0.4\ e/C_g$ and the temperature was fixed at $T = 0.09$ K when $V_b < 0$. When $V_b > 0$, the gate voltage was set between $V_g = 0.3\ e/C_g$ and $0.4\ e/C_g$, and $T = 0.13$ K. (We note that we had to change V_g to measure the TLF over the range of bias voltage.) The dashed and solid lines are simulations from the inelastic scattering and island self-heating models, respectively.

BROAD DISCUSSION

We can draw some very general conclusions from the switching data shown in Figs. 3–6. Clearly, $1/\tau_1$ and $1/\tau_2$ depend strongly on the bias conditions. In fact, the observed dependence is quite remarkable and not what one might naively expect. Consider, for example, Fig. 6, which shows how the two rates of $F2$ depend on the bias voltage across the SET. Naively one might expect that both transition rates should vary monotonically with V_b because both rates depend exponentially on the height of the energy barrier separating the two states and this height will vary monotonically when V_b is changed. Thus, the observed non-monotonic behavior of $1/\tau_1$ strongly suggests that barrier tilting is *not* the only significant factor which determines the switching dynamics.

To determine, in fact, which factors significantly affect the switching dynamics, it is crucial to know the location of the defect. By using Green's reciprocation theorem[14] to estimate the distance a charged defect must move to induce the observed island charge shift of $\Delta Q_o = 0.1 \pm 0.025\ e$,[15] we can say something about the location of the defect. From the theorem, one can show that the island charge shift is $\Delta Q_o = -q\mathbf{E} \cdot \Delta\mathbf{x}/\phi_i$ where $\mathbf{E}$ is the electric field at the location of the defect generated by an island potential ϕ_i when all other metal surfaces are grounded, q is the charge of the defect, and $\Delta\mathbf{x}$ is the displacement of the charge. If the defect has a charge $q = e$, is located in a junction with a 1 nm thick barrier, and the displacement is along the electric field, one finds $\Delta x \simeq 0.1$ nm. This is a reasonable distance for an ion or electron to move reversibly in a solid. In contrast, if $q = e$ and the defect is located at the outer surface of the SET island (modeled as a spherical island with a radius of 0.1 μm), then $\Delta x \simeq 10$ nm to cause the same charge shift $\Delta Q_o \simeq 0.1\ e$. This is unreasonably far for an ion or electron to switch back and forth repeatedly, suggesting that it is improbable that our TLF $F2$ is outside the tunnel junction if it is singly charged. We note that the induced polarization island charge shift caused by TLF $F1$ is even larger than that produced by $F2$ suggesting that it is also in the tunnel junction.

While our TLFs are most likely in the tunnel junction, we note that other published studies on charge noise in SETs have reported charge noise sources outside the tunnel junctions. For example, Zorin *et al.*[16] observed correlations between $1/f$ spectra from two nearby SETs and interpreted it as arising from moving background charges in the substrate. In another study, Zimmerman *et al.*[17] examined the gate voltage dependent behavior of what they concluded was a cluster of charges. They found the transition rate of the cluster was non-periodic in the gate voltage, strongly suggesting that the cluster was not in the junction.

Further evidence that our moving charge resides in the tunnel junction may be found in the temperature dependence of the transition rates of $F2$. From Fig. 3b, we concluded that the TLF is not in thermal equilibrium with the bath for all T. There are only a few ways this could happen. First, conduction electrons tunneling on and off the island cause fluctuations in the island potential ϕ_i which might couple to the fluctuator and "heat" it above T. A simple calculation, however, strongly suggests the fluctuating island potential cannot drive the TLF significantly from equilibrium. Suppose we model the defect as an ion with mass m_d which is connected via a spring with stiffness k_d to the insulator. Similarly, we can represent

the insulator as an infinite linear chain of masses with mass m and springs with stiffness k. Assuming that $m_d \approx m \approx m_{\text{oxygen}}$ and $k \approx 1\ eV/\text{Å}^2$, one can estimate that it takes $\tau_d \approx m_d/\sqrt{mk} \simeq 10^{-14}$ s (where k_d drops out) for the defect to relax back to equilibrium by emitting phonons. However, for our SET, $C_\Sigma = 0.126$ fF and the typical current through the device is a fraction of a nanoampere. This implies that fluctuations in the island potential occur on a time scale of about $\tau_i \simeq e/I \sim 10^{-10}$ s with an amplitude of about 1 mV. Because τ_d is several orders of magnitude shorter than τ_i, we do not expect the fluctuating island potential to disturb the TLF from equilibrium for a significant amount of time.[18] Changing the spring constant k by an order of magnitude or two does not affect this conclusion.

SELF-HEATING MODEL OF TWO-LEVEL FLUCTUATOR

Another mechanism which could possibly drive the fluctuator from equilibrium involves self-heating of the island due to the applied bias current. Although one might expect the heating to be very small because of the low power involved (typically a fraction of a picowatt), in fact the small volume of the island leads to very significant heating effects due to loss of good thermal contact between electrons and phonons at low temperatures.[19] One virtue of this mechanism is that it is largely amenable to calculations. Using the procedure outlined in R. L. Kautz *et al.*,[19] we calculate that the temperature of the transport electrons on the island never dropped below about 1 K when measuring the data presented in Fig. 3. Interestingly, the ratio τ_1/τ_2 deviates from a straight line (see Fig. 3b) at a temperature of about 0.7 K which suggests that the local region surrounding the defect could have been affected by the temperature of the conduction electrons on the island.

To better understand the influence island self-heating might have had on the transition rates, we constructed a simple model. We assume the defect is a charged particle with charge q which can switch between two wells separated by an energy barrier of height ε_b (see Fig. 7). To insure $\tau_2 < \tau_1$, we specify that the energy of state 2 is ΔE larger than that of state 1. The rate out of state 1 is given by:

$$\frac{1}{\tau_1} = \frac{1}{\tau_o} e^{-\varepsilon_b/(k_b T_d)}, \tag{1}$$

where $1/\tau_o$ is the attempt frequency out of state 1 and 2 and T_d is the temperature of the defect. Similarly, the rate out of state 2 is given by:

$$\frac{1}{\tau_2} = \frac{1}{\tau_o} e^{-(\varepsilon_b - \Delta E)/(k_b T_d)}. \tag{2}$$

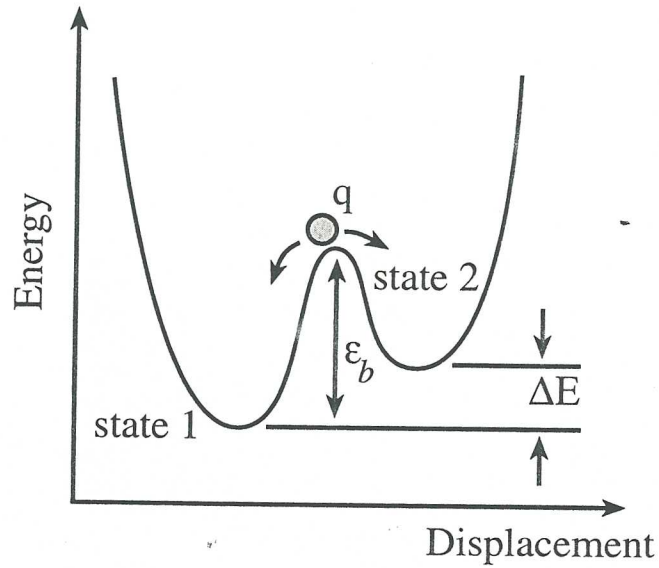

Fig. 7. Schematic of asymmetric double-well potential. The fluctuator is modeled as a particle with charge q which can be thermally activated over the barrier of height ε_b which separates the two states 1 and 2.

We assumed the same attempt frequency out of state 1 and 2 because as shown in Fig. 3b the ratio $\tau_2/\tau_1 \to 1$ as the bath temperature $T \to \infty$.

In our model, we assumed the temperature T_d of the defect was equal to the island electron temperature. The solid lines in Figs. 3, 4 and 6 show the results from the model which give the best fits to the data for TLF *F2*. The three fitting parameters $1/\tau_o$, ΔE, and ε_b are $1.7 \times 10^3\ \text{s}^{-1}$, 0.28 meV, and 0.49 meV, respectively. Examination of the plots shows that the best fit to the model agrees qualitatively with the three most striking features of the data: At low temperatures, the rates become temperature independent (see Fig. 3), (ii) the rates depend periodically on V_g (see Fig. 4), and (iii) $1/\tau_1$ is non-monotonic in V_b (see Fig. 6). This agreement is quite striking given the complexity of the data and the simplicity of the model. Even though the model contains just three fitting parameters, includes no potential tilting, and assumes the defect is at the temperature of the conduction electrons on the island, it fits the unexpected features of the data. We emphasize that the voltage dependence of the rates is hidden in the defect temperature T_d. This simple model suggests that island self-heating may be affecting the dynamics of the TLF.

On the other hand, despite the good qualitative agreement, the model shows significant quantitative disagreements. For example, in Fig. 3a the simulated rate $1/\tau_i$ saturates at a higher temperature than the data, resulting in a larger predicted ratio of the rates τ_2/τ_1 than the measured ratio in the low-temperature limit (see Fig. 3b). Moreover, the model predicts a sharp transition around 1 K; the predicted ratio τ_2/τ_1 follows a straight line above 1 K and suddenly becomes temperature independent below 1 K. In contrast, the measured ratio $\tau_2/\tau_1(T)$ exhibits a more gradual transition. In Fig. 4 the model shows a much lower maximum value for $1/\tau_2$ (when $Q_o \simeq -0.8\ e$, $0.2\ e$, and $1.2\ e$) and fails to predict the asymmetry of the peaks seen in the data. Also, in Fig. 6 the shape of the predicted $1/\tau_2(V_b)$ curve differs from the data, with the curve dropping nearly to zero as $|V_b| \to 0$. The measured data, however, seems to saturate around 130 s^{-1} as $V_b \to 0$. This suggests the model is missing some essential physics which would prevent $1/\tau_2$ from going to zero as $|V_b| \to 0$.

Clearly, while this model is simple and qualitatively agrees with some features of the data, the actual microscopic details are more complicated. Moreover, while the increase in the island temperature is plausible, the microscopic mechanism which allowed the temperature of the defect to increase significantly is unknown. In fact, it is difficult to imagine a coupling between the defect and the island conduction electrons which is strong enough to raise the defect temperature appreciably. Finally, we note that the model is unable to fit the $F1$ data shown in Fig. 5. The model predicts maximum transition rates when $Q_o = 0.5$. This clearly disagrees with the data, suggesting this defect may be of a different nature than the one discussed in Figs. 3, 4, and 6. Because of these weaknesses in the model, one should ask the question if there is another mechanism which could explain the data.

INELASTIC-SCATTERING MODEL OF TWO-LEVEL FLUCTUATOR

Another possible way to disturb the fluctuator, causing it to become out of equilibrium with the bath, is for electrons flowing through the SET to inelastically scatter from it. To see how inelastic scattering can affect the behavior of the charge fluctuations, we constructed a phenomenological model of the system. Like the self-heating model, the fluctuations are caused by a charged particle with charge q which can switch between two square wells which are separated by an energy barrier of height ε_b and width d_t (see Fig. 8a). To insure $\tau_2 < \tau_1$, we specify that the energy of state 2 is ΔE larger than that of state 1, again like the self-heating model. From the data, we know that $1/\tau_2$ never drops below about 130 s^{-1}. This is true

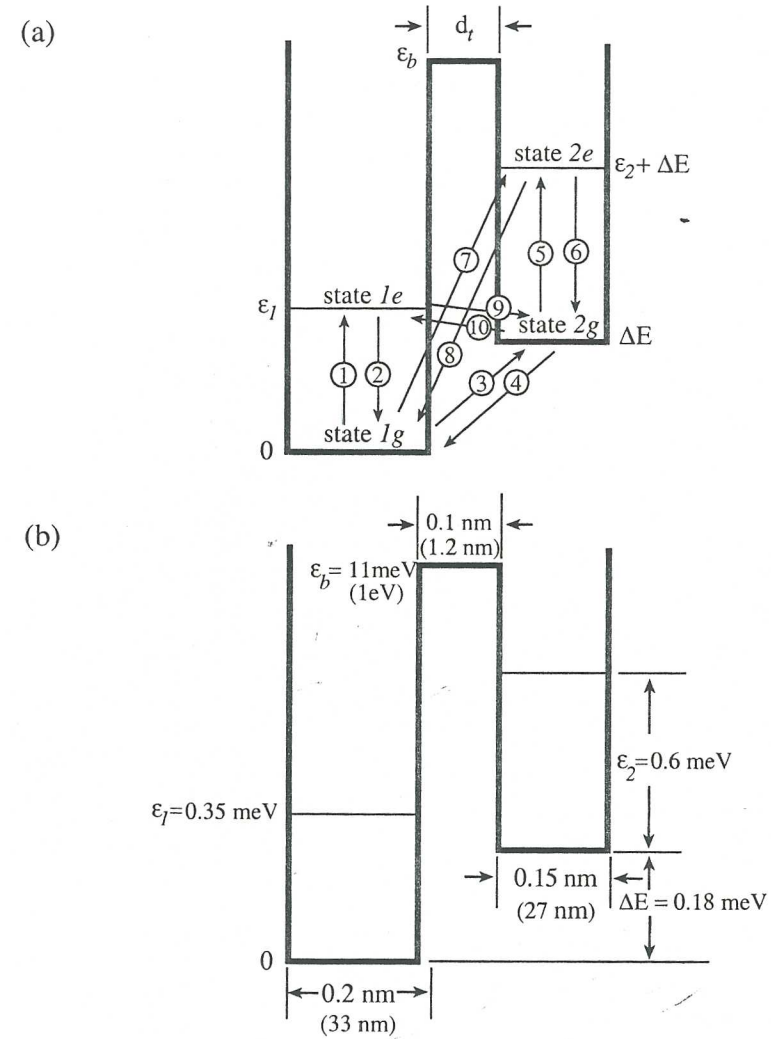

Fig. 8. Different transitions are possible between the two wells which are separated by a barrier with height ε_b and width d_t. The rates $\Gamma_{1g\to 1e} = \Gamma^{in}_{1g\to 1e} + \Gamma^{ab}_{1g\to 1e}$, $\Gamma^{em}_{1e\to 1g}$, $\Gamma^{ab}_{1g\to 2g}$, $\Gamma^{em}_{2g\to 1g}$, $\Gamma_{2g\to 2e} = \Gamma^{in}_{2g\to 2e} + \Gamma^{ab}_{2g\to 2e}$, $\Gamma^{em}_{2e\to 2g}$, $\Gamma^{ab}_{1g\to 2e}$, $\Gamma^{em}_{2e\to 1g}$, $\Gamma^{em}_{1e\to 2g}$, and $\Gamma^{em}_{2g\to 1e}$ correspond to 1, 2, 3, 4, 5, 6, 7, 8, 9, and 10, respectively. (b) Well dimensions and energy levels of the double-well potential inferred from the model. The widths of the wells are derived from ε_1 and ε_2 where we assume the charge is an oxygen ion. The well widths in parentheses are the values derived when we assume the charge is an electron. The tunnel barrier height ε_b for an oxygen ion is inferred from the fitting parameter $1/\tau_{1g\to 2e}$, the assumptions that $d_t = 0.1$ nm, and $m = m_o$. If we assume that $d_t = 0.3$ nm and $m = m_e$, then the height is much larger (value in parentheses).

even at low temperatures where there are relatively few phonons present and at low bias voltage where there are relatively few electrons to scatter off the charge. To explain these transitions, we assume that the defect can directly tunnel from the right well (state 2) to the left well (state 1) at a rate $\Gamma^{em}_{2g\to 1g}$ (see Table I). To conserve energy, we assume that after tunneling to the left well, the particle emits a single phonon and falls to the ground state in the left well, thus we use the superscript "*em*" to denote emission. The tunneling rate is proportional to a constant $1/\tau_{1g\rightleftharpoons 2g}$ which depends on the size of the barrier. We note that to enforce detailed balance, we must include the time-reversed process corresponding to the absorption of a phonon and a transition from the left to the right well at a rate $\Gamma^{ab}_{1g\to 2g}$ where the superscript "*ab*" denotes absorption (see Table I for explicit expressions for these and subsequent rates).

TABLE I

Individual Rates and Their Corresponding Physical Process. The Five Parameters $1/\tau_{1g\rightleftharpoons 2g}$, $1/\tau_{1g\rightleftharpoons 1e}$, $1/\tau_{1g\rightleftharpoons 2e}$, $1/\tau_{1e\rightleftharpoons 2g}$, and $1/\tau_{2g\rightleftharpoons 2e}$ are Constants. The Constants $1/\tau_{ig\rightleftharpoons ie}$ where $i=1$ or 2 Are Proportional to the Phonon Inelastic Scattering Cross-Section. The Other Parameters Are Tunneling Rates Through the Barrier. See Text for Explicit Form for $\Gamma^{in}_{ig\to ie}$ where $i=1$ or 2. The Numbers in Parentheses Correspond to the Circled Numbers in Fig. 8a

		Physical process
Process starting in left well		
(1)	$\Gamma^{ab}_{1g\to 1e}=\dfrac{1/\tau_{1g\rightleftharpoons 1e}}{e^{\beta\varepsilon_1}-1}$	absorption of phonon
(1)	$\Gamma^{in}_{1g\to 1e}$	electron inelastic scattering
(2)	$\Gamma^{em}_{1e\to 1g}=\dfrac{1/\tau_{1g\rightleftharpoons 1e}}{1-e^{-\beta\varepsilon_1}}$	emission of phonon
(3)	$\Gamma^{ab}_{1g\to 2g}=\dfrac{1/\tau_{1g\rightleftharpoons 2g}}{e^{\beta\Delta E}-1}$	tunneling and absorption of phonon
(7)	$\Gamma^{ab}_{1g\to 2e}=\dfrac{1/\tau_{1g\rightleftharpoons 2e}}{e^{\beta(\varepsilon_2+\Delta E)}-1}$	tunneling and absorption of phonon
(9)	$\Gamma^{em}_{1e\to 2g}=\dfrac{1/\tau_{1e\rightleftharpoons 2g}}{1-e^{-\beta(\varepsilon_1-\Delta E)}}$	tunneling and emission of phonon
Process starting in right well		
(5)	$\Gamma^{ab}_{2g\to 2e}=\dfrac{1/\tau_{2g\rightleftharpoons 2e}}{e^{\beta\varepsilon_2}-1}$	absorption of phonon
(5)	$\Gamma^{in}_{2g\to 2e}$	electron inelastic scattering
(4)	$\Gamma^{em}_{2g\to 1g}=\dfrac{1/\tau_{1g\rightleftharpoons 2g}}{1-e^{-\beta\Delta E}}$	tunneling and emission of phonon
(6)	$\Gamma^{em}_{2e\to 2g}=\dfrac{1/\tau_{2g\rightleftharpoons 2e}}{1-e^{-\beta\varepsilon_2}}$	emission of phonon
(8)	$\Gamma^{em}_{2e\to 1g}=\dfrac{1/\tau_{1g\rightleftharpoons 2e}}{1-e^{-\beta(\varepsilon_2+\Delta E)}}$	tunneling and emission of phonon
(10)	$\Gamma^{ab}_{2g\to 1e}=\dfrac{1/\tau_{1e\rightleftharpoons 2g}}{e^{\beta(\varepsilon_1-\Delta E)}-1}$	tunneling and absorption of phonon

Since the defect is charged, in general the energy splitting ΔE between wells will depend on the voltages applied to the SET. To include this effect, we assume that ΔE deviates from its untilted value ΔE_o by the expression:

$$\Delta E=\Delta E_o-0.1\ e(V_b-\phi_i), \tag{3}$$

where $\phi_i=(C_1V_b-ne+C_gV_g)/C_\Sigma$ is the island potential and n is the number of excess electrons on the island. The prefactor in the second term is determined from the fact that the measured shift in the island charge ΔQ_o equals 0.1 e. It is implicit in Eq. (3) that the defect is in the left tunnel junction, so that the potential at the defect lies between the island potential ϕ_i and the bias voltage V_b.

To complete the model, we add inelastic scattering between the charged particle and the electrons flowing through the SET. The only way we obtain a reasonable qualitative fit to our data is to assume that each well contains microstates. In particular, we assume that state 2 contains two microstates: a ground state ($2g$) and an excited state ($2e$), and they are separated by an energy ε_2. With this assumption, when an electron tunnels across the junction from state k in the electrode into state k' in the island, the charged particle can absorb energy ε_2. This inelastic scattering rate can be written as:

$$\Gamma^{in}_{2g\to 2e}=\frac{M_2}{e^2R_1}\int dE_k\,dE_{k'}\,f(E_k)(1-f(E_{k'}))\times\delta(E_k-E_{k'}-\Delta E_c-\varepsilon_2), \tag{4}$$

where M_2 is a constant proportional to the cross-section, $f(E)$ is the Fermi-Dirac distribution, and ΔE_c is the junction charging energy associated with the particular tunneling process.[20]

With the addition of microstates $2g$ and $2e$, there are some additional processes which must be included. If the fluctuator is excited into state $2e$, we assume it can emit a phonon and drop back into state $2g$ at a rate $\Gamma^{em}_{2e\to 2g}$. In this case, the current I would not switch. On the other hand, the charge could tunnel through the barrier into state 1 at a rate $\Gamma^{em}_{2e\to 1g}$, emitting a phonon in the process and causing an observable shift in the current. We note that we are forced by time-reversal symmetry to also put in a single-phonon absorption rate $\Gamma^{ab}_{2g\to 2e}$ for transitions from state $2g$ to state $2e$.

Our description for state 1 is very similar. We also assume that it is comprised of two microstates, a ground state (state $1g$) and an excited state (state $1e$) separated by an energy splitting ε_1. As with state 2, the charge can absorb a phonon and directly switch to state $2g$ at a rate $\Gamma^{ab}_{1g\to 2g}$, or it can be excited to state $1e$ by either a phonon or electron at a rate of $\Gamma^{ab}_{1g\to 1e}$ or $\Gamma^{in}_{1g\to 1e}$, respectively.[21] Once in state $1e$, the charge can drop back to state $1g$ at a rate $\Gamma^{em}_{1e\to 1g}$ in which case no change in current is observed and the process starts over, or it can tunnel across the barrier at a rate $\Gamma^{em}_{1e\to 2g}$, causing a switching event. Again, time-reversal symmetry forces us to include a rate $\Gamma^{ab}_{2g\to 1e}$ which corresponds to a direct transition where the defect absorbs a phonon and goes from state $2g$ to state $1e$.

The ten different transitions possible in the model are summarized in Fig. 8a. In order to determine the overall transition rate out of state 1 or 2 in terms of the individual rates, one has to solve the master equation[22] for the system. In general, the solution is complicated because of the different pathways the system can follow. It is instructive to look at the solution for $1/\tau_1$ for a simpler case where $\Gamma^{ab}_{1g\to 2g}=0$. For this case, one finds:

$$\frac{1}{\tau_1}=\frac{(\Gamma^{in}_{1g\to 1e}+\Gamma^{ab}_{1g\to 1e})\,\Gamma^{em}_{1e\to 2g}}{\Gamma^{in}_{1g\to 1e}+\Gamma^{ab}_{1g\to 1e}+\Gamma^{em}_{1e\to 1g}+\Gamma^{em}_{1e\to 2g}}. \tag{5}$$

Here, $1/\tau_1$ shows the typical rate behavior associated with a two-step series process. Note that if $\Gamma^{em}_{1e\to 2g}$ is much greater than the other rates, for instance, then $1/\tau_1 \simeq \Gamma^{in}_{1g\to 1e}+\Gamma^{ab}_{1g\to 1e}$, i.e., the rate $\Gamma^{in}_{1g\to 1e}+\Gamma^{ab}_{1g\to 1e}$ at which the charge gets to the excited state $1e$ is the rate limiting step.

Finally, we note that the individual rates depend on n, the number of excess electrons on the SET island. This happens because the island potential ϕ_i and the charging energy ΔE_c, are affected by n; ϕ_i affects the barrier height via tilting and ΔE_c affects the number of electrons which flow through the SET. In an SET, the number n fluctuates as electrons tunnel through the SET. Taking this into account, we can write the rate $1/\tau_i$ ($i=1$ or 2) as:

$$\frac{1}{\tau_i}=\sum_{n=-\infty}^{\infty}\frac{1}{\tau_i(n)}P(n), \tag{6}$$

where $P(n)$ is the probability that the island has n excess electrons,[19] and $1/\tau_i(n)$ is the solution to the master equation for this system when the charge starts in state ig where $i=1$ or 2. To evaluate Eq. (6), we fix V_g, V_b, and T, compute ϕ_i, ΔE_c, and $P(n)$ using the Orthodox Theory, and evaluate $\tau_i(n)$ using our model.[24]

COMPARISON BETWEEN MODEL AND DATA

Altogether there are ten undetermined parameters in our model: $1/\tau_{1g\rightleftharpoons 2g}$, $1/\tau_{1g\rightleftharpoons 1e}$, $1/\tau_{1g\rightleftharpoons 2e}$, $1/\tau_{1e\rightleftharpoons 2g}$, $1/\tau_{2g\rightleftharpoons 2e}$, ε_1, ε_2, M_1, M_2, and ΔE_0. However, the number of independent parameters drops to *two* for $1/\tau_1$ and *three* for $1/\tau_2$ for the bias and gate voltage data when $T\ll 1$ K. The dashed lines in Figs. 3, 4, and 6 show results from the model which give the best χ^2-fit to the $F2$ data and Table II contains the best fitting values. Examination of the plots shows that the best fit to the model agrees qualitatively with the three most striking features of the data: (i) At low temperatures, the rates become temperature independent (see Fig. 3), (ii) the rates depend periodically on V_g (see Fig. 4), and (iii) $1/\tau_1$ is non-monotonic in V_b (see Fig. 6). We have found that removing the tunneling transitions, inelastic scattering, or phonon driven transitions leads to a qualitatively poor agreement. However, if we remove tilting from the model by letting $\Delta E=\Delta E_o$ [see Eq. (3)], the fit does not change significantly, implying that barrier tilting may not be responsible for the periodic dependence of $1/\tau_1$ and $1/\tau_2$ on V_g.

Despite the good qualitative agreement, the model shows significant quantitative disagreements. For example, in Fig. 4 the model shows a much lower minimum value for $1/\tau_1$ (when $Q_o\simeq -0.2\ e$, $0.8\ e$, and $1.8\ e$) and fails to predict the asymmetry of the peaks seen in the data. Also, in Fig. 6 the shape of the predicted $1/(V_b)$ curve differs from the data, with the curve rising far above the data as $V_b\to 0$ for $V_b<0$ and dropping far below the data as $V_b\to 0$ for $V_b>0$. Finally, this model is unable to fit the $F1$ data shown in Fig. 5.

Although the model reproduces the main qualitative features in the data shown in Figs. 3, 4, and 6, the quantitative disagreements are significant. Such disagreements can occur, even though we have ten fitting parameters, because the data has so many non-trivial dependences and we made many simplifying assumptions. For example, we assumed the charge was moving in a simple 1-D potential like the one shown in Fig. 6a. The actual potential may be a more complicated 3-D potential. We also

TABLE II

Best Fit Model Parameters. Rows $i=1$ and $i=2$ Correspond to Transition Rates $1/\tau_1$ and $1/\tau_2$, Respectively.

Rate	$1/\tau_{1g\rightleftharpoons 2g}$ (s^{-1})	$1/\tau_{ig\rightleftharpoons ie}$ (s^{-1})	$1/\tau_{1e\rightleftharpoons 2g}$ (s^{-1})	$1/\tau_{1g\rightleftharpoons 2e}$ (s^{-1})	ε_i (meV)	M_i (e)	ΔE_o (meV)
$i=1$	130	1×10^9	130	—	0.35	0.175	0.23
$i=2$	130	7×10^8	—	2000	0.6	0.2	0.23

assumed the tunneling matrix elements between the wells were constants independent of the bias conditions. This is not necessarily true over the full range of bias conditions. We furthermore assumed that the single-phonon and conduction electron inelastic scattering cross-sections are constants, independent of the details of the potential's shape, the energy levels, or the incident energy of the scattering phonon or conduction electron. Finally, we assume that the Orthodox Theory[9] gives the correct values for $P(n)$. In our model, for some bias conditions small changes in $P(n)$ significantly change the calculated transition rates.

THE NATURE OF THE DEFECT: IS IT AN ION OR AN ELECTION?

Another test of the inelastic scattering model is the reasonableness of the fitting parameter values we found (see Table II). For example, if we assume that the defect is an oxygen ion with mass $m = m_o$ and the system acts like a particle-in-a-box, then the width l of the left well is $l = \sqrt{h^2/(8m_o\varepsilon_1)} = 0.2$ nm, where we use the value $\varepsilon_1 = 0.35$ meV found from fitting the model. This is a reasonable microscopic width for the well. Similarly, we can infer the width of the right well is $l = \sqrt{h^2/(8m_o\varepsilon_2)} = 0.15$ nm using $\varepsilon_2 = 0.6$ meV. Figure 8b summarizes these results.

We find that the other parameters are also reasonable. For example, if we assume that the charge is an oxygen atom tunneling through a rectangular potential barrier of width 0.1 nm, then from the tunneling rate $1/\tau_{1g \rightleftharpoons 2e}$, we can infer by using the WKB approximation[25] that the tunneling barrier has a height of about 11 meV (see Fig. 8b). Although this is a low energy barrier, we are clearly observing a very rare type of defect. Also, our best fit value $\sqrt{\varepsilon_b}\, d_t = 0.33$ $\sqrt{meV}$ nm agrees to within a factor of about 4 with the value reported by Rogers and Buhrman[8] in their study of resistance fluctuations in nanobridges. They also interpreted their two-level fluctuator data as supporting the idea of an ion hopping between two sites.

Finally, we can determine whether the values we obtained for the scaling factors M_1 and M_2 are sensible by comparing the inelastic scattering rate $\Gamma^{in}_{ia \rightarrow ib}$ ($i = 1$ and 2) to the total number of electrons flowing through the junction. Since we expect that each electron can at most generate one inelastic scattering event, we expect $\Gamma^{in}_{ia \rightarrow ib} < I/e$ where $i = 1$ or 2. From such a comparison, we find that the values $M_1 = 0.175$ and $M_2 = 0.20$ imply that not more than eighteen and twenty percent of the electrons flowing through the SET scatter off the TLF when the fluctuator is in state 1 and state 2, respectively. This is a large fraction of the total, but not unreasonable considering the small size of the junctions.

A natural question to ask is whether the random-telegraph noise could be due to a defect in the junction which is capturing and releasing electrons,

rather than due to the movement of an ion. A case against the charge being an electron trap can be made by considering the value we found for the tunneling rate $1/\tau_{1g \rightleftharpoons 2e} = 2000\ s^{-1}$. Since $Q_o = 0.1\ e$, the barrier thickness of the defect d_t cannot be more than a few angstroms. Using the WKB approximation[25] we can estimate that the tunnel barrier height would have to be about 80 eV, assuming the tunnel barrier width is about a lattice spacing $d_t = 0.3$ nm and the well width is also about a lattice spacing $l = 0.3$ nn. Clearly, this value for ε_b is far too large.

Another possibility is the charge fluctuations are caused by an electron moving back and forth between two sites. In this case, d_t could, in principle, be larger than in the electron trap case because the electron can move parallel and perpendicular to the electric field **E** in the junction. The measured value $\Delta Q_o = 0.1\ e$ only constrains the displacement of the electron parallel to **E** in the junction to a few angstroms; the displacement of the electron perpendicular to **E** could be greater than this. Thus, if $d_t = 1.2$ nm, for example, then $\varepsilon_b = 1$ eV which is entirely reasonable. However, if we assume that the charge has the mass of an electron $m = m_e$ and behaves like a particle-in-a-box, then we can infer that the width of the left well is $l = \sqrt{h_2/8m_e\varepsilon_1} = 33$ nm where we use $\varepsilon_1 = 0.35$ meV. This is much wider than the thickness of the junction barrier (see Fig. 8b).

We thus conclude that it is unlikely that the charge fluctuations are caused by the trapping and untrapping of an electron because the parameters of our model lead to unreasonable energy barriers. In contrast, the same model yields reasonable numbers when we assume the fluctuations are due to a singly charged ion or electron which is moving between two sites. If it is an electron moving, however, a simple particle-in-a-box picture is inconsistent with ε_1 and ε_2.

Inelastic scattering between transport electrons and charged defects is not a new idea in the study of random-telegraph noise. For example, in their study of resistance fluctuations in nanobridges, K. S. Ralls *et al.*[7] modeled the fluctuating system as a harmonic oscillator which exchanged energy with transport electrons. We note, however, that the specific model of K. S. Ralls *et al.*[7] does not explain our data if the defect is an ion; the model requires that the ion is heated out of equilibrium, which is implausible for our system as discussed above. Instead, we are proposing that inelastic scattering directly drives the fluctuator from one state to another.

CONCLUSIONS

We measured the transition rates of a single, charged two-level fluctuator as a function of the gate voltage V_g, the bias voltage V_b, and the

bath temperature T. Since that the ratio τ_2/τ_1 is not proportional to a Boltzmann factor, the fluctuator was not in equilibrium with the bath. We discuss two mechanisms which could disturb the defect from equilibrium with the bath, inelastic scattering between the defect and conduction electrons and island self-heating. While the defect, in principle, could be heated by the island conduction electrons anywhere near the island, it is most likely located in the tunnel junction because of the large magnitude of ΔQ_o.

We constructed a simple model of a charge moving in the junction which is heated by the island transport electrons. This model agrees qualitatively with our data, and explains the unusual features. The model suggests that charge noise in some SETs may be a result of delivering power to the island; the power delivered may heat the dielectrics nearby and cause charges to move more easily. However, the nature of the strong coupling between the defect and island conduction electrons necessary to raise the defect temperature significantly is difficult to imagine.

Our second phenomenological model of an ion or electron moving in the junction includes single-phonon scattering, conduction electron scattering, and quantum tunneling. This model agrees qualitatively with our data, and explains the main unusual features. Although the model simplifies the microscopic details of the defect and its interactions with the environment, we are able to discern from the values of the fitting parameters that the defect is either an ion hopping a distance of about 0.1 nm between two localized sites separated by a barrier of height $\simeq 11$ meV, or an electron moving about 1 nm between two sites which are separated by a barrier of height roughly equal to 1 eV. It is difficult to reconcile our data with the picture of an electron trapping and untrapping. Finally, we note that the model suggests that charge noise in some SETs may be a result of applying bias current to the device; the conduction electrons flowing through the SET drive charge motion in the tunnel barriers. Further study of more devices is necessary to generalize these results and determine the extent to which island self-heating and inelastic scattering contribute to charge noise.

ACKNOWLEDGMENTS

This work was supported by NIST, Gaithersburg, and the state of Maryland through the Center for Superconductivity Research. We wish to acknowledge Alan F. Clark and E. R. Williams for many useful discussions.

REFERENCES

1. J. M. Martinis, M. Nahum, and Hans Dalsgaard Jenson, *Phys. Rev. Lett.* **72**, 904 (1994).
2. A. F. Clark, N. M. Zimmerman, E. R. Williams, A. Amar, D. Song, F. C. Wellstood, C. J. Lobb, R. J. Soulen, Jr., *Appl. Phys. Lett.* **66**, 2588 (1995).

3. K. Nakazato, R. J. Blaike, J. R. A. Cleaver, and H. Ahmed, *Electron. Lett.* **29**, 384 (1993).
4. Alexander Shnirman, Gerd Shön, and Ziv Hermon, *Phys. Rev. Lett.* **79**, 2371 (1997).
5. Y. Nakamura, Yu. A. Pashkin, and J. S. Tsai, *Nature* **398**, 786 (1999).
6. K. S. Ralls, W. J. Skocpol, L. D. Jackel, R. E. Howard, L. A. Fetter, R. W. Epworth, and D. M. Tennant, *Phys. Rev. Lett.* **52**, 228 (1984).
7. K. S. Ralls, D. C. Ralph, and R. A. Buhrman, *Phys. Rev. B* **40**, 11561 (1989).
8. C. T. Rogers and R. A. Buhrman, *Phys. Rev. Lett.* **55**, 859 (1985).
9. D. V. Averin and K. K. Likharev, in *Mesoscopic Phenomena in Solids* edited by B. Al'tshuler, P. A. Lee, and R. A. Webb (Elsevier, Amsterdam, 1991), p. 173.
10. G. J. Dolan, *Appl. Phys. Lett.* **31**, 337 (1977).
11. We used powder microwave filters at the mixing chamber; see for example, J. M. Martinis, Ph.D. thesis (University of California, Berkeley, 1985), p. 22.
12. For details of our fabrication process, the experimental procedure we used to determine the $I-V_g-V_b$ characteristics, and the method we used to find device parameters, see M. Kenyon, A. Amar, D. Song, C. J. Lobb, and F. C. Wellstood, *Appl. Phys. Lett.* **72**, 2268 (1998).
13. The experiment was done in a single run on the dilution refrigerator which lasted for about two weeks. During this time the defect was reasonably stable as the data reflects.
14. D. Song, A. Amar, C. J. Lobb, and F. C. Wellstood, *IEEE Trans Appl. Supercond.* **5**, 3085 (1995). William R. Smythe, in *Static and Dynamic Electricity* (Taylor and Francis, Bristol, PA, 1989).
15. We found that ΔQ_o was practically independent of V_b, V_g, and T.
16. A. B. Zorin, F. J. Ahlers, J. Niemeyer, T. Weimann, H. Wolf, V. A. Krupenin, S. V. Lotkhov, *Phys. Rev. B* **53**, 13682 (1995).
17. Neil M. Zimmerman, Jonathan L. Cobb, and Alan F. Clark, *Phys. Rev. B* **56**, 7675 (1997).
18. F. Reif, in *Fundamentals of Statistical and Thermal Physics* (McGraw–Hill, New York, 1965), p. 573.
19. R. L. Kautz, G. Zimmerli, and John M. Martinis, *J. Appl. Phys.* **73**, 2386 (1993).
20. For forward tunneling, the number of electrons on the island changes from n to $n+1$, and the charging energy is:

$$\Delta E_c = \frac{e^2}{2C_\Sigma}\left(2\left(n-\frac{C_g V_g}{e}\right)+1\right)+eV_b\frac{(C_2+C_g)}{C_\Sigma},$$

where $C_\Sigma = C_1 + C_2 + C_g$. For backward tunneling, n changes from n to $n-1$, and the charging energy is:

$$\Delta E_c = -\frac{e^2}{2C_\Sigma}\left(2\left(n-1-\frac{C_g V_g}{e}\right)+1\right)-eV_b\frac{(C_2+C_g)}{C_\Sigma}.$$

See M. Tinkham, in *Introduction to Superconductivity*, 2nd ed. (McGraw–Hill, New York, 1996), p. 278.
21. The rate $\Gamma^{in}_{1g\to 1e}$ is similar to $\Gamma^{in}_{2g\to 2e}$. We write it as:

$$\Gamma^{in}_{1g\to 1e} = \frac{M_1}{e^2 R_1}\int dE_k\, dE_{k'}\, f(E_k)(1-f(E_{k'}))\times\delta(E_k - E_{k'} - \Delta E_c - \varepsilon_1).$$

M_1 is an overall scaling factor, proportional to the cross-section and ε_1 is the energy splitting between thate $1g$ and state $1e$. The other terms in these two equations are explained in the discussion following Eq. (4).
22. We do not include transitions between the excited states $1e$ and $2e$ in the model. Including such transitions will not significant effect the results of the model. The model also does not include inelastic scattering between the defect and the electrons flowing through the SET which cause direct transitions between the left and the right wells. Including these processes will introduce more fitting parameters and improve the fit. However, the qualitative behavior of the model will not change.

23. Harry S. Robertson, in *Statistical Thermophysics* (Prentice–Hall, New Jersey, 1993), p. 440.
24. We note the model also includes the uncertainty in the island charge Q_o due to the movement of other background charges. By measuring the $1/f$ charge noise at $T_b = 0.1$ K, we determined that the uncertainty in Q_o was $\Delta Q_o \simeq 0.03\ e$. Therefore, when we calculate $1/\tau_i(n)$, we perform a weighted average over V_g which reflected this uncertainty in Q_o.
25. To determine ε_b from $1/\tau_{1g \rightleftharpoons 2e}$, we use the following equations:

$$1/\tau_{1g \rightleftharpoons 2e} = \frac{\sqrt{2m\varepsilon_2}}{2ml} \exp\left(-\frac{2}{h}\sqrt{2m\varepsilon_b}\, d_r\right),$$

where we assume $d_r = 0.1$ nm, $m = m_o$ the mass of an oxygen ion, and $l = 0.2$ nm is the width of the right well. See R. Shankar, in *Principles of Quantum Mechanics*, 2nd ed. (Plenum Press, New York, 1994), p. 445.

Journal of Low Temperature Physics, Vol. 123, Nos. 1/2, 2001

Effect of Voltage Bias on the dc SQUID Characteristics

M. Kiviranta* and H. Seppä

VTT Automation, Measurement Technology, Otakaari 7B, 02150 Espoo, Finland

(Received May 12, 2000; revised December 12, 2000)

The dynamics of the dc SQUID, when voltage biased through an inductor, is computed by numerical simulation and by perturbative analytical calculation. We find that the dynamic resistance decreases from its current-biased value at low bias voltages, where the inductive series reactance no longer separates the Josephson voltage oscillation from the bias source. The flux-to-current conversion ratio, however, remains almost unaffected. This effect is sometimes important in setups, where a second SQUID is used as a readout amplifier.

1. INTRODUCTION

Operation of SQUIDS with voltage bias rather than current bias has certain advantages and has gained popularity recently. When a second SQUID is used as a preamplifier in the SQUID readout, it is natural to voltage bias the first SQUID and measure its current.[1] When positive flux feedback is used to facilitate the direct coupling to the room-temperature preamplifier, voltage bias allows larger dynamic range and in practice easier opearation than current bias.[2,3] Furthermore, use of voltage bias makes it possible to relax the requirements for junction damping, which can be utilized to develop lower-noise devices.[4] Use of voltage bias, however, leads to modified dynamics and IV characteristics at low voltages, when compared with the current-biased case.

Ultimately one is interested in the case where the thermal noise of the shunt resistors is taken into account. This case has been considered in conjunction with current-biased SQUIDS by various authors,[5,6] but to the authors' knowledge the effect of the voltage bias has not been treated. The current paper considers the noiseless characteristics.

*E-mail: mikko.kiviranta@vtt.fi